Structural Engineering and Mechanics, *Vol. 60, No. 2 (2016) 175-191*
DOI: http://dx.doi.org/10.12989/sem.2016.60.2.175

Moving load response on the stresses produced in an irregular microstretch substrate

Tanupreet Kaur*[1], Satish Kumar Sharma[1a], Abhishek Kumar Singh[2b] and Mriganka Shekhar Chaki[2c]

[1]*School of Mathematics, Thapar University, Patiala-147004, Punjab, India*
[2]*Department of Applied Mathematics, Indian School of Mines, Dhanbad-826004, Jharkhand, India*

(Received March 4, 2016, Revised June 7, 2016, Accepted June 10, 2016)

Abstract. The present article is aimed at an investigation of stresses produced in a microstretch elastic half-space due to a moving load. The expressions of normal stress, shear stress and tangential couple stress produced in this case have been obtained in closed form. To find the displacement fields the perturbation method is applied. Significant effect of moving load on variation of stresses developed at different depths below the surface due to the depth of substrate and frictional coefficient of the rough surface of the medium has been observed. The effects of different shapes of irregularity and depth of irregularity on normal, shear and tangential couple stresses have been discussed. Some particular cases have also been deduced from the present investigation. Finally, the analytical developments have been illustrated numerically for aluminium-epoxy-like material substrate under the action of moving load.

Keywords: moving load; microstretch; frictional coefficient; irregularity; stresses

1. Introduction

Microstretch model can be used as a mathematical model for many different material media like chopped elastic fibers, porous media whose pores are filled with gas or inviscid liquid, asphalt and solid-liquid crystals which fall outside the domain of micropolar elasticity (which can model human bones, chopped fiber composites, platelet composites, porous material, foams, bones). This microstructured continua possesses internal expansion and contraction (breathing) modes independent of their transformations and rotations, in addition to the micropolar modes. Microstretch elastic solids possess seven degrees of freedom: three for translation, three for rotation and one for stretch. When directors are rigid there are only three rotational degrees of freedom in addition to three classical displacement degrees of freedom and the Microstretch theory is reduced to micropolar theory. Further, if the directors are taken to be fully coupled to the material points, the rotational degree of freedom of micropolar theory become equal to classical

*Corresponding author, Ph.D. Student, E-mail: tanupreet12@gmail.com
[a]Ph.D., E-mail: satishk.sharma@thapar.edu
[b]Ph.D., E-mail: abhi.5700@gmail.com
[c]Ph.D. Studnet, E-mail: mriganka.chaki@gmail.com

http://www.techno-press.org/?journal=sem&subpage=8 ISSN: 1225-4568 (Print), 1598-6217 (Online)

rotations and micropolar theory reduces to couple stress theory. When the particle reduces to the mass point, all the theories reduce to classical continuum mechanics. The theory of microstretch elastic solid was introduced by Eringen (1971) as a special case of micromorphic theory in addition to generalization of micropolar theory. Iesan and Pompei (1995) discussed the boundary value problems of the equilibrium theory of homogeneous and isotropic solids. Tomar and Garg (2005) investigated the reflection and transmission from a plane interface between two microstretch elastic solid half-spaces. Forest and Sievert (2006) presented a hierarchy of higher order continua by introducing additional degrees of freedom. Sharma *et al*. (2007) studied the Rayleigh surface waves propagation in microstretch thermoelastic continua under inviscid fluid loadings. Sharma and Kumar (2016) studied the influence of microstructure, heterogeneity and internal friction on SH-waves propagation in a viscoelastic layer overlying a couple stress substrate.

The stress developed in body due to moving load causing fracture is an interesting problem of mechanics having its applications towards the stability of the medium. The response of a moving load over a surface is a subject of investigation because of its possible practical application in determining the strength of a structure. The physical problem of a fracture is a dynamic problem in which the slip has to be considered as a consequence of stress conditions and the strength of material in the focal region. From this point of view, the mechanism of an earthquake is represented by a shear fracture produced by the drop in stress in the focal region. Fracture initiates at a point of the fault when the stress acting on the fault plane exceeds a critical value, propagates with a certain velocity, and finally stops when conditions impede its further propagation. Cole and Huth (1958) obtained the steady state solution of the problem of moving load over an elastic half space and Craggs (1960) derived a relatively simple closed-form solution, exhibiting a resonance effect at a critical load velocity, which in this case equals the velocity of Rayleigh waves. Earlier, Sneddon (1952) has studied the problem considered by Cole and Huth (1958) but with different solution strategy. Mukherjee (1969) has studied the stresses developed in a transversely isotropic elastic half-space due to normal moving load over a rough surface. The problem of moving load on a plate resting on a layered half space has been solved by Sackman (1961) and Miles (1966). Some notable work concerned with the problem of moving load on an elastic half-space has been done by Achenbach *et al*. (1967), Chonan (1976), Ungar(1976), Olsson (1991), Lee and Ng (1994), Alkeseyeva (2007) etc. The problem of a normal load over a transversely isotropic layer lying on rigid foundation is investigated by Mukhopadhyay (1965) whereas Selim (2007) discussed the static deformation of an irregular initially stressed medium. He used the Eigen value approach to solve the problem. The dynamic response of a normal moving load in the plane of symmetry of a monoclinic half-space was studied by Chattopadhyay *et al*. (2006). Chattopadhyay *et al*. (2011) have also studied the stress on a rough irregular isotopic half-space due to normal moving load. Effect of irregularity and heterogeneity on the stresses produced due to a normal moving load on a rough monoclinic half-space has been studied by Singh *et al*. (2014). The response of moving load on a micropolar half-space with irregularity is investigated by Kaur *et al*. (2015). Szylko-Bigus and niady (2015) presented dynamic analysis of Timoshenko beams under continuous moving load. Due to moving load the structural damage and force identification was studied by Zu *et al*. (2015). Kaur *et al*. (2016) analyzed dynamic response of normal moving load on an irregular fiber-reinforced half-space. Elastic solutions due to a time-harmonic point load in isotropic multi-layered media has been investigated by Lin *et al*. (2016).

The theory of microstretch elastic solids is a further generalization of the theory of micropolar elasticity. Since such a generalized media can catch more detailed information about the micro-

deformation inside a material point, which is more suitable for modeling the overall property of the composite materials reinforced with chopped elastic fibers and various porous solids, it has drawn the attention of many researchers for investigation. Although, the earlier studies had shown that the stress developed due to a moving load and the effect of the presence of irregularity in a media have a great utilization in the interpretation and analysis of geophysical fracture, yet, no attempts has been made to study the stresses developed in an irregular microstretch substrate due to a normal moving load. In the present problem, not only the induced stresses due to moving load on microstretch media has been investigated but also the effect of irregularity on induced stresses has been studied and this serves as a novel feature to the present problem with respect to the existing works available in the literature.

The present problem is concerned with the effect of a moving load on the surface of microstretch elastic substrate with irregularity. The closed form expressions for the stresses produced at any point of the microstretch elastic substrate due to inclined load are obtained. To find the displacement fields the perturbation method is applied. The effects of friction of the rough surface and irregularity in the substrate have been studied by introducing frictional coefficient (R) and irregularity factor (x/a). To study the effect of irregularity, in the substrate, the variation of stresses with depth have been drawn.

2. Formulation of the problem

We consider a model which consists of a microstretch elastic substrate with parabolic irregularity under the influence of normal moving load F which is independent of y and moving with a constant velocity V in the direction of positive x-axis. The rectangular Cartesian co-ordinate system is introduced having origin at the middle point of span of the irregularity and y-axis pointing vertically downwards as shown in Fig. 1.

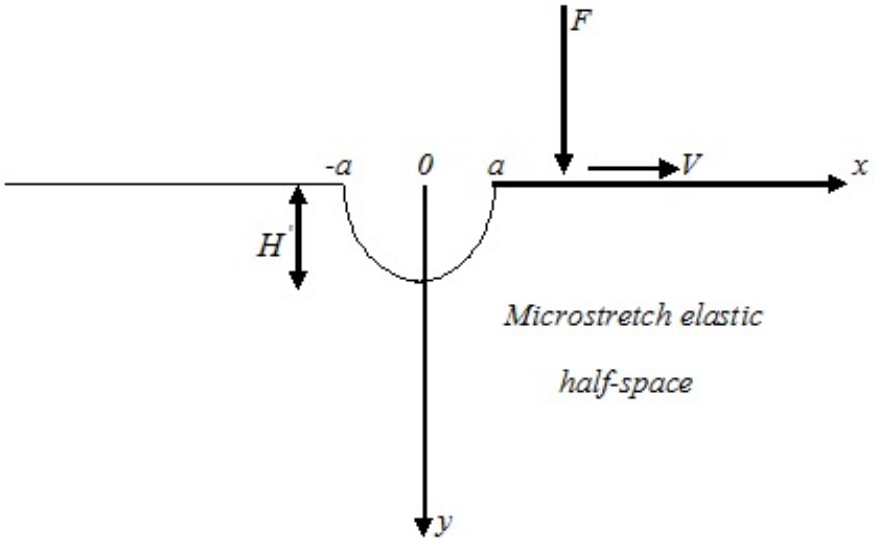

Fig. 1 Geometry of the problem

The equation of upper interface containing irregularity is

$$y = \varepsilon h(x), \tag{1}$$

where

$$h(x) = \begin{cases} 0, & |x| \geq a \\ \dfrac{2\left(a^2 - x^2\right)}{a}, & |x| < a \end{cases}$$

and $\varepsilon = \dfrac{H'}{2a} << 1$, is a small positive number, H' is the maximum depth of the irregularity below the interface and *2a* is the span of the irregularity.

The basic governing equation of motion and constitutive relations in microstretch elastic substrate, in the absence of body force are given by Eringen (1990)

$$(\mu + \kappa)\nabla^2 \vec{u} + (\lambda + \mu)\nabla\left(\nabla.\vec{u}\right) + \kappa\left(\nabla \times \vec{\phi}\right) + \lambda_0 \nabla \phi^* = \rho \frac{\partial^2 \vec{u}}{\partial t^2}, \tag{2}$$

$$(\alpha + \beta + \gamma)\nabla\left(\nabla.\vec{\phi}\right) - \gamma\nabla \times \left(\nabla \times \vec{\phi}\right) + \kappa\left(\nabla \times \vec{u}\right) - 2\kappa\vec{\phi} = \rho j \frac{\partial^2 \vec{\phi}}{\partial t^2}, \tag{3}$$

$$\frac{2}{3}\alpha_0 \nabla^2 \phi^* - \frac{2}{9}\lambda_1 \phi^* - \frac{2}{9}\lambda_0\left(\nabla.\vec{u}\right) = \rho j \frac{\partial^2 \phi^*}{\partial t^2}, \tag{4}$$

$$\sigma_{ij} = \lambda u_{r,r}\delta_{il} + \mu\left(u_{i,l} - u_{l,i}\right) + \kappa\left(u_{l,i} - \varepsilon_{ilr}\phi_r\right) + \lambda_0 \delta_{ij}\phi^*, \tag{5}$$

$$m_{il} = \alpha\phi_{r,r}\delta_{il} + \beta\phi_{i,l} + \gamma\phi_{l,i}, \tag{6}$$

where $\vec{u}, \vec{\phi}$ and $\overrightarrow{\phi^*}$ are displacement, microrotation and microstretch functions respectively.

Here $\lambda, \mu, \kappa, \alpha, \beta, \gamma, \alpha_0, \lambda_0$ and λ_1 are material constants, ρ is the density of the material, j is microinertia, σ_{il} and m_{il} are the stress tensor and couple stress tensor respectively and δ_{il} is the Kronecker delta.

For two-dimensional problem, we assume

$$\vec{u} = (u, v, 0) \; and \; \vec{\phi} = (0, 0, \phi).$$

The equations of motion (2), (3) and (4) can be written as

$$(\lambda + 2\mu + \kappa)\frac{\partial^2 u}{\partial x^2} + (\mu + \kappa)\frac{\partial^2 u}{\partial y^2} + (\lambda + \mu)\frac{\partial^2 v}{\partial x \partial y} + \kappa\frac{\partial \phi}{\partial y} + \lambda_0 \frac{\partial \phi^*}{\partial x} = \rho \frac{\partial^2 u}{\partial t^2}, \tag{7}$$

$$(\lambda + 2\mu + \kappa)\frac{\partial^2 v}{\partial y^2} + (\mu + \kappa)\frac{\partial^2 v}{\partial x^2} + (\lambda + \mu)\frac{\partial^2 u}{\partial x \partial y} - \kappa\frac{\partial \phi}{\partial x} + \lambda_0 \frac{\partial \phi^*}{\partial y} = \rho \frac{\partial^2 v}{\partial t^2}, \tag{8}$$

$$\gamma\left(\frac{\partial^2 \phi}{\partial x^2} + \frac{\partial^2 \phi}{\partial y^2}\right) + \kappa\left(\frac{\partial v}{\partial x} - \frac{\partial u}{\partial y}\right) - 2\kappa\phi = \rho j \frac{\partial^2 \phi}{\partial t^2}, \tag{9}$$

$$\frac{2}{3}\alpha_0\left(\frac{\partial^2\phi^*}{\partial x^2}+\frac{\partial^2\phi^*}{\partial y^2}\right)-\frac{2}{9}\lambda_1\phi^*-\frac{2}{9}\lambda_0\left(\frac{\partial u}{\partial x}+\frac{\partial v}{\partial y}\right)=\rho j\frac{\partial^2\phi^*}{\partial t^2}. \tag{10}$$

The boundary conditions at $y=\varepsilon h(x)$ may be written as

$$\sigma_{yy}=-F\delta\left(x-Vt\right), \tag{11}$$

$$\sigma_{yx}=-FR\delta\left(x-Vt\right), \tag{12}$$

$$m_{xz}=0, \tag{13}$$

$$\frac{\partial\phi^*}{\partial x}=0, \tag{14}$$

where m_{xz} is tangential couple stress, σ_{yy} and σ_{yx} are normal and shearing stresses and $\delta(x)$ is Dirac delta function and $\delta\left(x-Vt\right)=\frac{1}{\pi}\int_0^\infty\cos k\left(x-Vt\right)dk.$

3. Solution of the problem

The solution of equations of motion (7), (8), (9) and (10) may be assumed as

$$u=\int_0^\infty\left[Ae^{-\omega qy}\cos\left(\omega\left(x-Vt\right)\right)+Be^{-\omega qy}\sin\left(\omega\left(x-Vt\right)\right)\right]d\omega, \tag{15}$$

$$v=\int_0^\infty\left[Ce^{-\omega qy}\cos\left(\omega\left(x-Vt\right)\right)+De^{-\omega qy}\sin\left(\omega\left(x-Vt\right)\right)\right]d\omega, \tag{16}$$

$$\phi=\int_0^\infty\omega\left[Ee^{-\omega qy}\cos\left(\omega\left(x-Vt\right)\right)+Fe^{-\omega qy}\sin\left(\omega\left(x-Vt\right)\right)\right]d\omega, \tag{17}$$

$$\phi^*=\int_0^\infty\omega\left[Ge^{-\omega qy}\cos\left(\omega\left(x-Vt\right)\right)+He^{-\omega qy}\sin\left(\omega\left(x-Vt\right)\right)\right]d\omega, \tag{18}$$

where ω is the wave number and q is independent of ω.

The form of assumed solutions (15)-(18) may be recognized to present a steady state solutions.

Using solutions given in Eqs. (15), (16), (17) and (18) in equations of motion (7), (8), (9) and (10), we have

$$\left[\left(\mu+\kappa\right)q^2+\rho V^2-\left(\lambda+2\mu+\kappa\right)\right]A-\left(\lambda+\mu\right)qD-\kappa qE+\lambda_0H=0, \tag{19}$$

$$\left[\left(\mu+\kappa\right)q^2+\rho V^2-\left(\lambda+2\mu+\kappa\right)\right]B+\left(\lambda+\mu\right)qC-\kappa qF-\lambda_0G=0, \tag{20}$$

$$\left[\left(\lambda+2\mu+\kappa\right)q^2+\rho V^2-\left(\mu+\kappa\right)\right]C-\left(\lambda+\mu\right)qB-\kappa F-\lambda_0qG=0, \tag{21}$$

$$\left[\left(\lambda+2\mu+\kappa\right)q^2+\rho V^2-\left(\mu+\kappa\right)\right]D+\left(\lambda+\mu\right)qA+\kappa E-\lambda_0qH=0, \tag{22}$$

$$\kappa D + \kappa qA - 2\kappa E = 0, \tag{23}$$

$$-\kappa C + \kappa qB - 2\kappa F = 0, \tag{24}$$

$$\lambda_1 G + \lambda_0 B - \lambda_0 qC = 0, \tag{25}$$

$$-\lambda_1 H + \lambda_0 A + \lambda_0 qD = 0, \tag{26}$$

$$\left[\rho jV^2 - \gamma\left(1-q^2\right)\right]E = 0, \tag{27}$$

$$\left[\rho jV^2 - \gamma\left(1-q^2\right)\right]F = 0, \tag{28}$$

$$\left[\rho jV^2 - \frac{2}{3}\alpha_0\left(1-q^2\right)\right]G = 0, \tag{29}$$

$$\left[\rho jV^2 - \frac{2}{3}\alpha_0\left(1-q^2\right)\right]H = 0, \tag{30}$$

Solving Eqs. (23)-(30), we get following relations

$$D = mA, C = -mB, E = \alpha A, F = \alpha B, G = -\beta B, H = \beta A \text{ and } V^2 = \frac{\gamma\left(1-q^2\right)}{\rho j},$$

where

$$\alpha = \frac{m+q}{2}, \beta = \lambda_0 \frac{qm+1}{\lambda_1}.$$

Using these relations in Eqs. (19) and (20), we get

$$m = \frac{\left(\mu + \frac{\kappa}{2}\right)q^2 + \frac{\lambda_0^2}{\lambda_1} + \rho V^2 - \left(\lambda + 2\mu + \kappa\right)}{\left(\lambda + \mu + \frac{\kappa}{2} - \frac{\lambda_0^2}{\lambda_1}\right)q}. \tag{31}$$

Similarly, from Eqs. (21) and (22), we get

$$m = \frac{\left(\lambda + \mu + \frac{\kappa}{2} - \frac{\lambda_0^2}{\lambda_1}\right)q}{\left(\lambda + \mu + \frac{\kappa}{2} - \frac{\lambda_0^2}{\lambda_1}\right)q^2 + \rho V^2 - \mu - \frac{\kappa}{2}}. \tag{32}$$

From Eqs. (31) and (32), we get

$$q^2 = \frac{Q \pm \sqrt{Q^2 - 4P^2}}{2P}, \tag{33}$$

where

$$P=\left(\mu+\frac{\kappa}{2}-\frac{\gamma}{j}\right)\left(\lambda+2\mu+\kappa-\frac{\lambda_0^2}{\lambda_1}-\frac{\gamma}{j}\right),$$

$$Q=\left(\mu+\frac{\kappa}{2}-\frac{\gamma}{j}\right)^2+\left(\lambda+2\mu+\kappa-\frac{\lambda_0^2}{\lambda_1}-\frac{\gamma}{j}\right)^2+\left(\lambda+\mu+\frac{\kappa}{2}-\frac{\lambda_0^2}{\lambda_1}\right)^2.$$

In view of equation (33), equations (15), (16), (17) and (18) can be written as

$$u=\int_0^\infty\left[\left(A_1e^{-\omega q_1y}+A_2e^{-\omega q_2y}\right)\cos\left(\omega\left(x-Vt\right)\right)+\left(B_1e^{-\omega q_1y}+B_2e^{-\omega q_2y}\right)\sin\left(\omega\left(x-Vt\right)\right)\right]d\omega, \quad (34)$$

$$v=\int_0^\infty\left[\left(B_1m_1e^{-\omega q_1y}+B_2m_2e^{-\omega q_2y}\right)\cos\left(\omega\left(x-Vt\right)\right)-\left(A_1m_1e^{-\omega q_1y}+A_2m_2e^{-\omega q_2y}\right)\sin\left(\omega\left(x-Vt\right)\right)\right]d\omega, \quad (35)$$

$$\phi=\int_0^\infty\omega\left[\left(\alpha_1A_1e^{-\omega q_1y}+\alpha_2A_2e^{-\omega q_2y}\right)\cos\left(\omega\left(x-Vt\right)\right)+\left(\alpha_1B_1e^{-\omega q_1y}+\alpha_2B_2e^{-\omega q_2y}\right)\sin\left(\omega\left(x-Vt\right)\right)\right]d\omega, \quad (37)$$

where

$$\alpha_1=\frac{m_1+q_1}{2},\alpha_2=\frac{m_2+q_2}{2},\beta_1=\lambda_0\frac{\left(q_1m_1+1\right)}{\lambda_1}\text{ and }\beta_2=\lambda_0\frac{\left(q_2m_2+1\right)}{\lambda_1}.$$

Now, setting the approximations due to small value of ε as follows:

$$A_1\cong A_{10}+\varepsilon A_{11},A_2\cong A_{20}+\varepsilon A_{21,}B_1\cong B_{10}+\varepsilon B_{11},B_2\cong B_{20}+\varepsilon B_{21}.$$

The terms A_1, A_2, B_1 and B_2 appearing in Eqs. (34), (35), (36) and (37) are functions of ε as the boundary is not uniform. These terms can be expanded in ascending powers of ε. Since ε is small, therefore, retaining the terms up to the first order of ε, we can approximate A_1, A_2, B_1 and B_2 as taken in the above assumption.

Moreover, for small ε the assumption $e^{\pm\varepsilon\nu h}\cong1\pm\varepsilon\nu h$ also holds well, where v is any quantity. Applying boundary conditions (11), (12), (13) and (14) on (34), (35), (36) and (37), we get

$$\left(\lambda-\lambda_0\beta_1\right)B_{10}+\left(\lambda-\beta_2\lambda_0\right)B_{20}=-\frac{F}{\pi\omega}, \quad (38)$$

$$\left(\lambda-\lambda_0\beta_1\right)A_{10}+\left(\lambda-\beta_2\lambda_0\right)A_{20}=0, \quad (39)$$

$$\left(\lambda-\lambda_0\beta_1\right)B_{11}+\left(\lambda-\beta_2\lambda_0\right)B_{21}-\left(\lambda-\lambda_0\beta_1\right)\omega q_1hB_{10}-\left(\lambda-\beta_2\lambda_0\right)\omega q_2hB_{20}=0, \quad (40)$$

$$\left(\lambda-\lambda_0\beta_1\right)A_{11}+\left(\lambda-\beta_2\lambda_0\right)A_{21}-\left(\lambda-\lambda_0\beta_1\right)\omega q_1hA_{10}-\left(\lambda-\beta_2\lambda_0\right)\omega q_2hA_{20}=0, \quad (41)$$

$$\xi_1A_{10}+\xi_2A_{20}=-\frac{FR}{\pi\omega}, \quad (42)$$

$$\xi_1B_{10}+\xi_2B_{20}=0, \quad (43)$$

$$\xi_1A_{11}+\xi_2A_{21}-\omega q_1h\xi_1A_{10}-\omega q_2h\xi_2A_{20}=0, \quad (44)$$

$$\xi_1 B_{11} + \xi_2 B_{21} - \omega q_1 h \xi_1 B_{10} - \omega q_2 h \xi_2 B_{20} = 0, \tag{45}$$

$$\alpha_1 B_{10} + \alpha_2 B_{20} = 0, \tag{46}$$

$$\alpha_1 A_{10} + \alpha_2 A_{20} = 0, \tag{47}$$

$$\alpha_1 B_{11} + \alpha_2 B_{21} - \alpha_1 \omega q_1 h B_{10} - \alpha_2 \omega q_2 h B_{20} = 0, \tag{48}$$

$$\alpha_1 A_{11} + \alpha_2 A_{21} - \alpha_1 \omega q_1 h A_{10} - \alpha_2 \omega q_2 h A_{20} = 0, \tag{49}$$

$$\beta_1 A_{10} + \beta_2 A_{20} = 0, \tag{50}$$

$$\beta_1 B_{10} + \beta_2 B_{20} = 0, \tag{51}$$

$$\beta_1 A_{11} + \beta_2 A_{21} - \omega q_1 h \beta_1 A_{10} - \omega q_2 h \beta_2 A_{20} = 0, \tag{52}$$

$$\beta_1 B_{11} + \beta_2 B_{21} - \omega q_1 h \beta_1 B_{10} - \omega q_2 h \beta_2 B_{20} = 0, \tag{53}$$

where

$$\xi_1 = q_1 (\kappa - \mu) + m_1 \mu - \kappa \alpha_1, \xi_1 = q_2 (\kappa - \mu) + m_2 \mu - \kappa \alpha_2.$$

Solving above equations, we get

$$A_{10} = \frac{FR\beta_2}{\pi\omega\xi_7}, A_{20} = -\frac{FR\beta_1}{\pi\omega\xi_7}, B_{10} = \frac{F\alpha_2}{\pi\omega\xi_8}, B_{20} = -\frac{F\alpha_1}{\pi\omega\xi_8}, A_{11} = \frac{FRh\xi_9}{\pi}, A_{21} = \frac{FRh\xi_{10}}{\pi}, B_{11} = \frac{Fh\xi_{11}}{\pi}, B_{21} = \frac{Fh\xi_{12}}{\pi}, \tag{54}$$

Where ξ_9, ξ_{10}, ξ_{11} and ξ_{12} are given in Appendix 1.

With the help of obtained values displacement components given in Eqs. (34), (35), (36) and (37) can be written as

$$\begin{aligned} u = F\int_0^\infty \Bigg[& \left(\frac{R\beta_2}{\pi\omega\xi_7} + \varepsilon h \frac{R\xi_9}{\pi} \right) e^{-\omega q_1 y} \cos\omega(x - Vt) + \left(-\frac{R\beta_1}{\pi\omega\xi_7} + \varepsilon h \frac{R\xi_{10}}{\pi} \right) e^{-\omega q_2 y} \cos\omega(x - Vt) \\ & + \left(\frac{\alpha_2}{\pi\omega\xi_8} + \varepsilon h \frac{\xi_{11}}{\pi} \right) e^{-\omega q_1 y} \sin\omega(x - Vt) + \left(-\frac{\alpha_1}{\pi\omega\xi_8} + \varepsilon h \frac{\xi_{12}}{\pi} \right) e^{-\omega q_2 y} \sin\omega(x - Vt) \Bigg] d\omega, \end{aligned} \tag{55}$$

$$\begin{aligned} v = F\int_0^\infty \Bigg[& \left(\frac{\alpha_2}{\pi\omega\xi_8} + \varepsilon h \frac{\xi_{11}}{\pi} \right) m_1 e^{-\omega q_1 y} \cos\omega(x - Vt) + \left(-\frac{\alpha_1}{\pi\omega\xi_8} + \varepsilon h \frac{\xi_{12}}{\pi} \right) m_2 e^{-\omega q_2 y} \cos\omega(x - Vt) \\ & - \left(\frac{R\beta_2}{\pi\omega\xi_7} + \varepsilon h \frac{R\xi_9}{\pi} \right) m_1 e^{-\omega q_1 y} \sin\omega(x - Vt) + \left(-\frac{R\beta_1}{\pi\omega\xi_7} + \varepsilon h \frac{R\xi_{10}}{\pi} \right) m_2 e^{-\omega q_2 y} \sin\omega(x - Vt) \Bigg] d\omega, \end{aligned} \tag{56}$$

$$\begin{aligned} \phi = F\int_0^\infty \omega \Bigg[& \alpha_1 \left(\frac{R\beta_2}{\pi\omega\xi_7} + \varepsilon h \frac{R\xi_9}{\pi} \right) e^{-\omega q_1 y} \cos\omega(x - Vt) + \alpha_2 \left(-\frac{R\beta_1}{\pi\omega\xi_7} + \varepsilon h \frac{R\xi_{10}}{\pi} \right) e^{-\omega q_2 y} \cos\omega(x - Vt) \\ & + \alpha_1 \left(\frac{\alpha_2}{\pi\omega\xi_8} + \varepsilon h \frac{\xi_{11}}{\pi} \right) e^{-\omega q_1 y} \sin\omega(x - Vt) + \alpha_2 \left(-\frac{\alpha_1}{\pi\omega\xi_8} + \varepsilon h \frac{\xi_{12}}{\pi} \right) e^{-\omega q_2 y} \sin\omega(x - Vt) \Bigg] d\omega, \end{aligned} \tag{57}$$

$$\phi^* = F\int_0^\infty \omega\Bigg[-\beta_1\left(\frac{R\beta_2}{\pi\omega\xi_7}+\varepsilon h\frac{R\xi_9}{\pi}\right)e^{-\omega q_1 y}\cos\omega\left(x-Vt\right)-\beta_2\left(-\frac{R\beta_1}{\pi\omega\xi_7}+\varepsilon h\frac{R\xi_{10}}{\pi}\right)e^{-\omega q_2 y}\cos\omega\left(x-Vt\right)$$
$$+\beta_1\left(\frac{\alpha_2}{\pi\omega\xi_8}+\varepsilon h\frac{\xi_{11}}{\pi}\right)e^{-\omega q_1 y}\sin\omega\left(x-Vt\right)+\beta_2\left(-\frac{\alpha_1}{\pi\omega\xi_8}+\varepsilon h\frac{\xi_{12}}{\pi}\right)e^{-\omega q_2 y}\sin\omega\left(x-Vt\right)\Bigg]d\omega, \tag{58}$$

Using expressions of displacement components from Eqs. (55) and (56); expression of microrotation function from Eq. (57); and microstretch function from Eq. (58) in Eqs. (5) and (6) which after performing integration result in the following expressions of non-vanishing stresses as

$$\frac{\sigma_{yy}}{F}=\frac{1}{\pi}\Bigg[-\left(\lambda-\lambda_0\beta_1\right)\left[\frac{R\beta_2}{\xi_7\phi_1}\left(x-Vt\right)+\frac{\alpha_2 q_1 y}{\xi_8\phi_1}\right]+\left(\lambda-\lambda_0\beta_2\right)\left[\frac{R\beta_1}{\xi_7\phi_2}\left(x-Vt\right)-\frac{\alpha_1 q_2 y}{\xi_8\phi_2}\right]$$
$$+\varepsilon h\Bigg(-\left(\lambda-\lambda_0\beta_1\right)\left[R\xi_9\frac{2q_1 y\left(x-Vt\right)}{\phi_1}+\xi_{11}\frac{\phi_3}{\phi_1^2}\right]+\left(\lambda-\lambda_0\beta_2\right)\left[R\xi_{10}\frac{2q_2\left(x-Vt\right)}{\phi_2}+\xi_{12}\frac{\phi_4}{\phi_2^2}\right]\Bigg)\Bigg], \tag{59}$$

$$\frac{\sigma_{yx}}{F}=\frac{1}{\pi}\Bigg[\left(\frac{\xi_1\alpha_2}{\xi_8\phi_1}+\frac{\xi_2\alpha_1}{\xi_8\phi_2}\right)\left(x-Vt\right)-\frac{R\xi_1\beta_2 q_1 y}{\xi_7\phi_1}+\frac{R\xi_2\beta_1 q_2 y}{\xi_7\phi_2}$$
$$+\varepsilon h\left(\left(-\xi_1\xi_{11}\frac{2q_1 y}{\phi_1^2}-\xi_2\xi_{12}\frac{2q_2 y}{\phi_2^2}\right)\left(x-Vt\right)+R\xi_1\xi_9\frac{\phi_3}{\phi_1^2}-R\xi_2\xi_{10}\frac{\phi_4}{\phi_1^2}\right)\Bigg], \tag{60}$$

$$\frac{m_{xz}}{F}=\frac{\gamma}{\pi}\Bigg[\left(-\frac{2R\alpha_1\beta_2 q_1 y}{\xi_7\phi_1^2}-\frac{2R\alpha_2\beta_1 q_2 y}{\xi_7\phi_2^2}\right)\left(x-Vt\right)+\frac{\alpha_1\alpha_2\phi_3}{\xi_8\phi_1^2}-\frac{\alpha_1\alpha_2\phi_4}{\xi_8\phi_2^2}+\varepsilon h\Bigg[2\alpha_1\xi_{11}\frac{q_1 y\left(\phi_3+2\left(x-Vt\right)^2\right)}{\phi_1^3}$$
$$+2\alpha_2\xi_{12}\frac{q_2 y\left(\phi_4+2\left(-Vt\right)^2\right)}{\phi_2^3}-2R\left(\alpha_1\xi_9\frac{2q_1^2y^2+\phi_3}{\phi_1^3}+\alpha_2\xi_{10}\frac{2q_2^2y^2+\phi_4}{\phi_2^3}\right)\Bigg]\Bigg], \tag{61}$$

where

$$\phi_1=q_1^2y^2+\left(x-Vt\right)^2,\phi_2=q_2^2y^2+\left(x-Vt\right)^2,\ \phi_3=q_1^2y^2-\left(x-Vt\right)^2,\phi_4=q_2^2y^2-\left(x-Vt\right)^2.$$

From Eqs. (60), (61) and (62), it is clear that the whole stress system is moving with uniform velocity *V* in the *x*-direction. The expression of stresses shows that in any plane lying below the free boundary surface and parallel to the *xz*-plane, the stresses attains maximum value at $x=Vt$, i.e., at the point directly below the point of application of the moving load with velocity V at time t. In further discussion we shall deal with the stresses at $x=Vt$.

4. Particular cases

4.1 Case 1

In the absence of irregularity effect (ε=0), the expression of stresses (59), (60) and (61) reduces to

$$\frac{\sigma_{yy}}{F}=\frac{1}{\pi}\left[-\left(\lambda-\lambda_0\beta_1\right)\frac{\alpha_2}{\xi_8 q_1 y}-\left(\lambda-\lambda_0\beta_2\right)\frac{\alpha_1}{\xi_8 q_2 y}\right], \tag{62}$$

$$\frac{\sigma_{yx}}{F}=-\frac{1}{\pi}\left[\frac{R\xi_1\beta_2}{\xi_7 q_1 y}+\frac{R\xi_2\beta_1}{\xi_7 q_2 y}\right], \tag{63}$$

$$\frac{m_{xz}}{F}=\frac{\gamma}{\pi}\left[\frac{\alpha_1\alpha_2}{\xi_8 q_1^2 y^2}-\frac{\alpha_1\alpha_2}{\xi_8 q_2^2 y^2}\right]. \tag{64}$$

Eqs. (62), (63) and (64) give the expression for normal, shear and tangential couple stresses respectively, produced due to normal moving load on a regular microstretch substrate.

4.2 Case 2

In the absence of stretch effect (λ_0=0 and α_0=0), the expression of stresses (59), (60) and (61) reduces to

$$\frac{\sigma_{yy}}{F}=\frac{\lambda}{\pi}\left[\frac{\alpha_2'}{\xi_8' q_1' y}-\frac{\alpha_1'}{\xi_8' q_2' y}+\varepsilon h\left(-\frac{\xi_{11}'}{q_1'^2 y^2}+\frac{\xi_{12}'}{q_2'^2 y^2}\right)\right], \tag{65}$$

$$\frac{\sigma_{yx}}{F}=0, \tag{66}$$

$$\frac{m_{xz}}{F}=\frac{\gamma}{\pi}\left[\frac{\alpha_1'\alpha_2'}{\xi_8' q_1'^2 y^2}-\frac{\alpha_1'\alpha_2'}{\xi_8' q_2'^2 y^2}+\varepsilon h\left(2\alpha_1'\xi_{11}'\frac{1}{q_1'^2 y^2}+2\alpha_2'\xi_{12}'\frac{1}{q_2'^2 y^2}\right)\right], \tag{67}$$

Eqs. (65), (66) and (67) are the expression for stresses produced due to normal moving load on an irregular micropolar substrate.

4.3 Case 3

In the absence of stretch and irregularity effects (λ_0=0, α_0=0 and ε=0), the expression of stresses (59), (60) and (61) reduces to

$$\frac{\sigma_{yy}}{F}=\frac{\lambda}{\pi}\left[\frac{\alpha_2'}{\xi_8' q_1' y}-\frac{\alpha_1'}{\xi_8' q_2' y}\right], \tag{68}$$

$$\frac{\sigma_{yx}}{F}=0, \tag{69}$$

$$\frac{m_{xz}}{F}=\frac{\gamma}{\pi}\left[\frac{\alpha_1'\alpha_2'}{\xi_8' q_1'^2 y^2}-\frac{\alpha_1'\alpha_2'}{\xi_8' q_2'^2 y^2}\right], \tag{70}$$

where $\alpha_1^{'}, \alpha_2^{'}, q_1^{'}, q_2^{'}$ and $\xi_8^{'}$ are provided in Appendix 2. Eqs. (68), (69) and (70) are the expression for stresses produced due to normal moving load on a regular micropolar substrate.

4.4 Case 4

In the absence of micropolar effect (λ_0=0, α_0=0, α=0, β=0, κ=0 and $\gamma\to 0$), the expression of stresses (65), (66) and (67) reduces to

$$\frac{\sigma_{yy}}{F} = \frac{\lambda}{\pi}\left[\frac{\alpha_2^{"}}{\xi_8^{"}q_1^{"}y} - \frac{\alpha_1^{"}}{\xi_8^{"}q_2^{"}y} + \varepsilon h\left(-\frac{\xi_{11}^{"}}{q_1^{"2}y^2} + \frac{\xi_{12}^{"}}{q_2^{"2}y^2}\right)\right], \tag{71}$$

$$\frac{\sigma_{yx}}{F} = 0, \tag{72}$$

$$\frac{m_{xz}}{F} = \frac{\gamma}{\pi}\left[\frac{\alpha_1^{"}\alpha_2^{"}}{\xi_8^{"}q_1^{"2}y^2} - \frac{\alpha_1^{"}\alpha_2^{"}}{\xi_8^{"}q_2^{"2}y^2} + \varepsilon h\left(2\alpha_1^{"}\xi_{11}^{"}\frac{1}{q_1^{"2}y^2} + 2\alpha_2^{"}\xi_{12}^{"}\frac{1}{q_2^{"2}y^2}\right)\right], \tag{73}$$

where $\alpha_1^{"}, \alpha_2^{"}, q_1^{"}, q_2^{"}$ and $\xi_8^{"}$ are provided in Appendix 3.

Eqs. (71), (72) and (73) are the expression for stresses produced due to normal moving load on an irregular isotropic substrate.

4.4 Case 5

In the absence of micropolar and irregularity effects(λ_0=0, α_0=0, α=0, β=0, κ=0, $\gamma\to 0$ and ε=0), the expression of stresses (65), (66) and (67) reduces to

$$\frac{\sigma_{yy}}{F} = \frac{\lambda}{\pi}\left[\frac{\alpha_2^{"}}{\xi_8^{"}q_1^{"}y} - \frac{\alpha_1^{"}}{\xi_8^{"}q_2^{"}y}\right], \tag{74}$$

$$\frac{\sigma_{yx}}{F} = 0, \tag{75}$$

$$\frac{m_{xz}}{F} = \frac{\gamma}{\pi}\left[\frac{\alpha_1^{"}\alpha_2^{"}}{\xi_8^{"}q_1^{"2}y^2} - \frac{\alpha_1^{"}\alpha_2^{"}}{\xi_8^{"}q_2^{"2}y^2}\right], \tag{76}$$

Eqs. (74), (75) and (76) are the expression for stresses produced due to normal moving load on a regular isotropic elastic substrate.

5. Numerical results

For sake of numerical computation and graphical demonstration, we have taken Aluminium-Epoxy-like material whose physical data is given by Singh and Kumar (1998)

$$\rho = 2.19\times10^3\, Kg/m^3, \lambda = 7.59\times10^{10}\, N/m^2, \mu = 1.89\times10^{10}\, N/m^2, \kappa = 0.0149\times10^{10}\, N/m^2,$$

$$\gamma = 0.268\times10^6\, N,\ j = 0.196\times10^4\, m^2, \lambda_0 = \lambda_1 = 0.37\times10^{10}\, N/m^2, \alpha_0 = 0.61\times10^{-9}\, N.$$

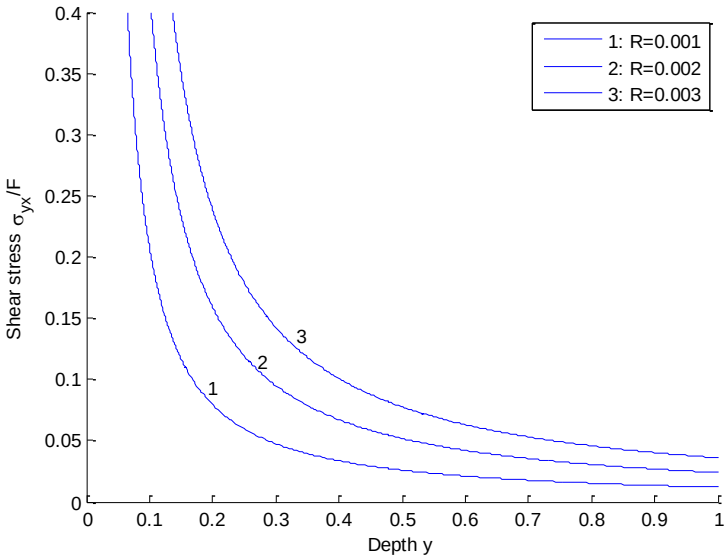

Fig. 2 Variation of the shear stress against depth for different values of frictional coefficients (R)

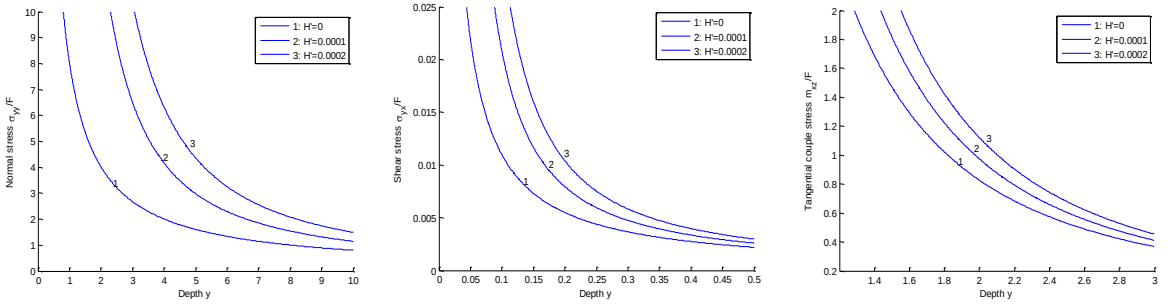

(a) (b) (c)

Fig. 3 Variation of the normal stress (in 3(a)), shear stress (in 3(b)) and tangential couple stress (in 3(c)) against depth for different values of irregularity depth (H'/a) when irregularity factor, x/a=0.5

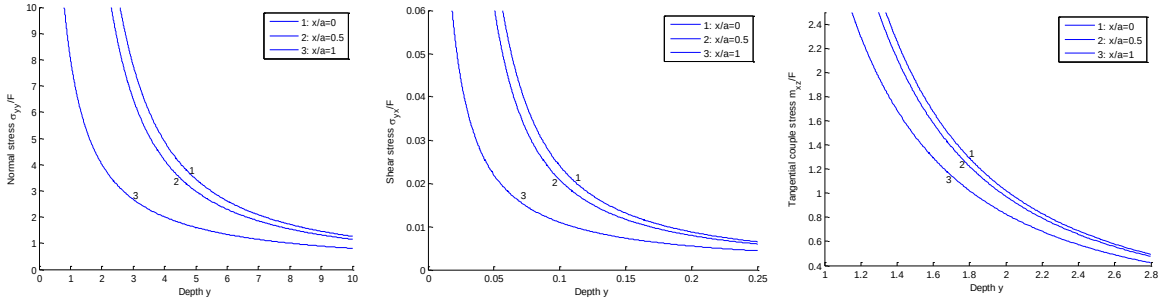

(a) (b) (c)

Fig. 4 Variation of the normal stress (in 4(a)), shear stress (in 4(b)) and tangential couple stress (in 4(c)) against depth for different values of irregularity factor (x/a) when irregularity depth, H'/a=1

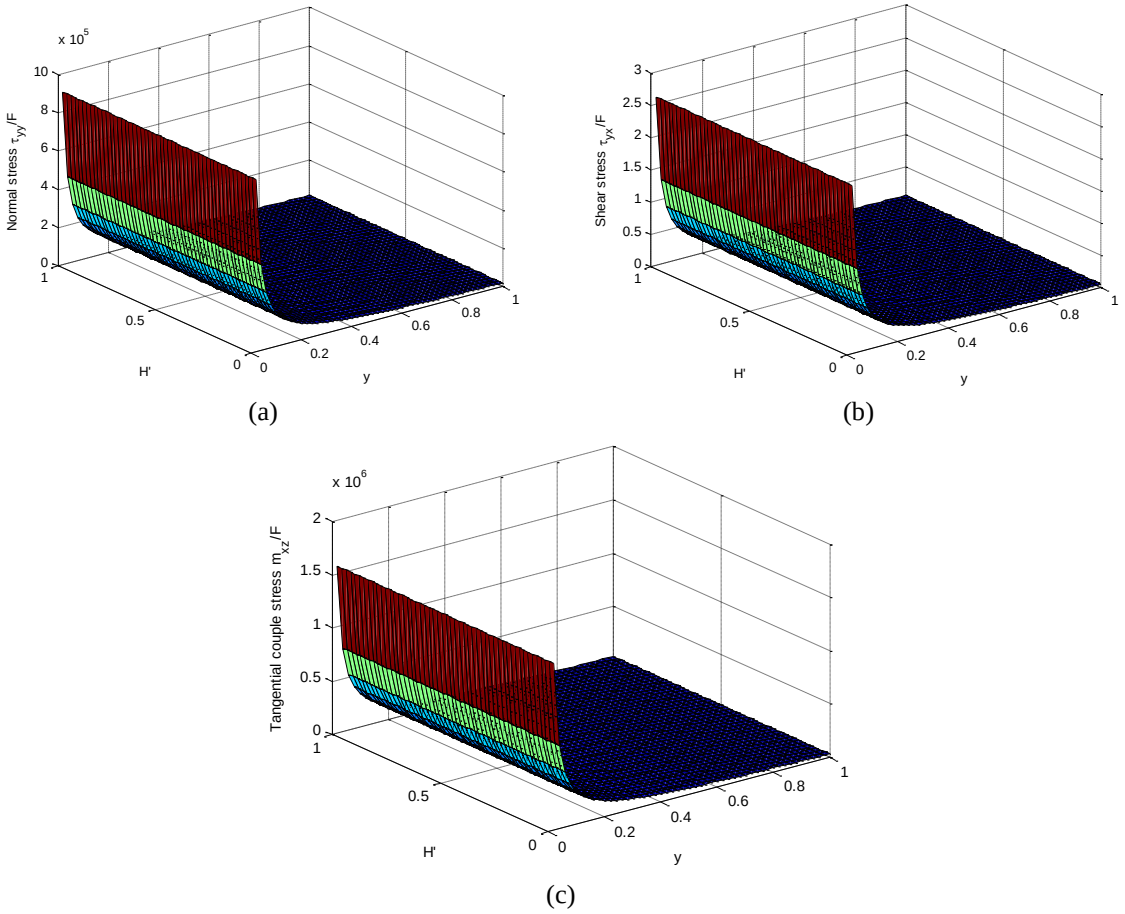

Fig. 5 Variation of the normal stress (in 5(a)), shear stress (in 5(b)) and tangential couple stress (in 5(c)) against depth and irregularity depth (H'/a) in case of rectangular irregularity

The variation of normal stress σ_{yy}/F, shear stress σ_{yx}/F and tangential couple stress m_{xz}/F in a microstretch elastic substrate for different values of frictional coefficient, depth of irregularity and different types of irregularity has been depicted by means of graphs (Figs. 2 to 6). Each of these figures manifests that with increase in depth of substrate all the three stresses decreases.

Fig. 2 depicts the effect of frictional coefficient of the free surface of microstretch elastic substrate on shear stress. Different values of frictional coefficient has been taken into account. For the considered values of frictional coefficient it has been observed from this figure that the frictional coefficient affects the shear stress predominately which increases with increase in frictional coefficient. It has also been found that in the expressions of normal stress (59) and tangential couple stress (61) both normal stress and tangential couple stress are independent of frictional coefficient. Therefore, variation of normal stress and tangential couple stress against depth are not plotted for different values of frictional coefficient.

The impact of different values of irregularity depth on normal stress, shear stress and tangential couple stress has been reflected in Figs. 3(a), 3(b) and 3(c). Curve 1 in these figures (Fig. 3) represents the case when there is no irregularity in the substrate whereas as curves 2 and 3 in these

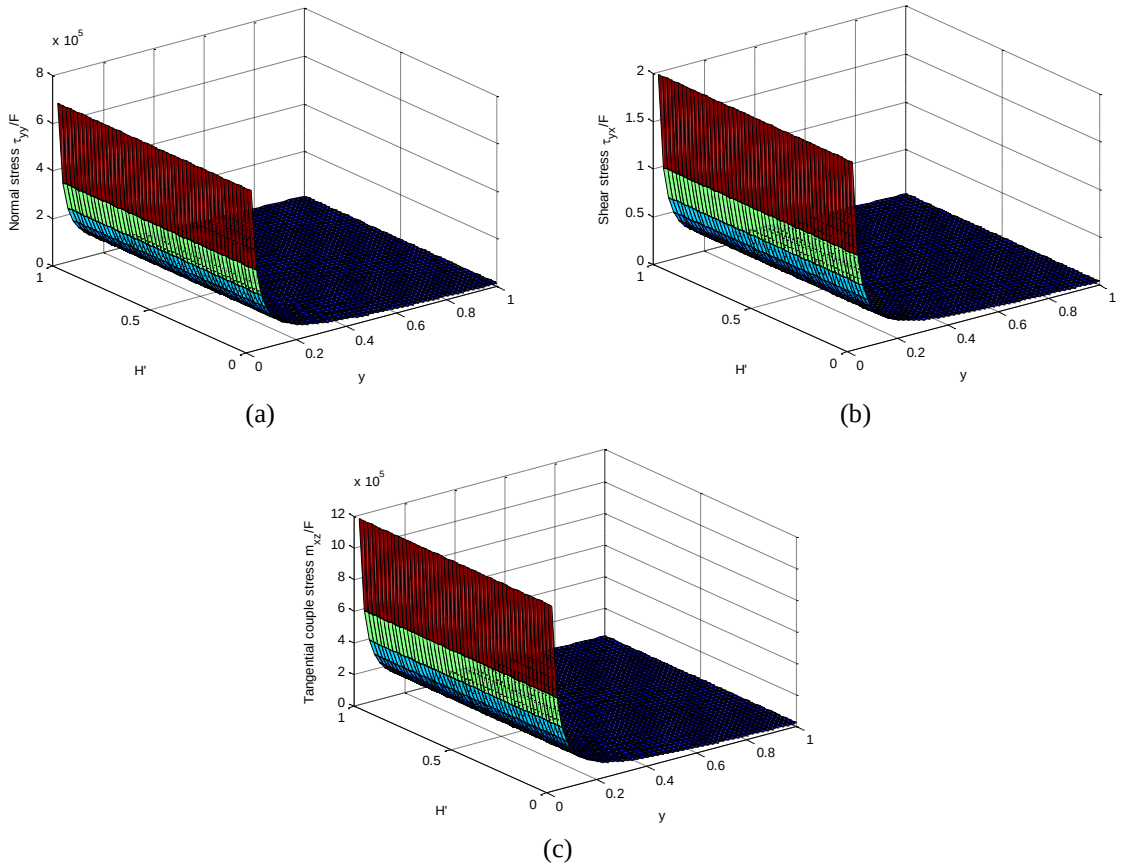

Fig. 6 Variation of the normal stress (in 6(a)), shear stress (in 6(b)) and tangential couple stress (in 6(c)) against depth and irregularity depth (H'/a) in case of parabolic irregularity

figures correspond to the case when there is irregularity in the substrate. It is evident from these figures that depth of irregularity has significant effect on all the three stresses i.e. all the three stresses increases with increase in depth of irregularity.

In Figs. 4(a), 4(b) and 4(c), curves have been drawn to study the impact of different types of irregularity viz. rectangular, parabolic and no irregularity on variation of normal stress, shear stress and tangential couple stress. Different values of irregularity factor has been taken for different types of irregularity. Curve 1 in these figures (Fig. 4) corresponds to the case when irregularity is of rectangular type, curve 2 represents the case of parabolic irregularity and curve 3 represents the case when surface is free from irregularity i.e., no irregularity. It is noticed from these figures that stresses are more in case of rectangular irregularity than the case of parabolic irregularity. More precisely, as the irregularity prevails in the medium stress increases.

Variation of normal stress, shear stress and tangential couple stress against irregularity depth and depth of substrate has been shown through surface plots in Fig. 5 and Fig. 6. If we compare surface plot in Fig. 5(a) with Fig. 6(a), Fig. 5(b) with Fig. 6(b) and Fig. 5(c) with Fig. 6(c), we observe that all the three stresses are favoured more with rectangular irregularity as compare to parabolic irregularity.

6. Conclusions

The stresses produced in an irregular microstretch substrate due to a normal moving load at a rough free surface have been investigated in the present study. Significant effects of depth of substrate, frictional coefficient of rough surface, maximum depth of irregularity and irregularity factor have been observed on stresses in a microstretch substrate. Three different types of irregularity has been considered and discussed viz. rectangular, parabolic and no irregularity. Closed form of expressions for the normal stress, shear stress and tangential couple stress have been obtained. The following points can be highlighted as an outcome of the study:

- Depth has a significant effect on the stresses. Stresses are more near the surface and magnitude decay as we go deep in the substrate i.e., stresses decreases with increase in the depth.
- It is observed that the frictional coefficient of the rough surface have notable effect on the shear stress. With increasing value of the frictional coefficient the shear stress increases, whereas the normal stress and tangential couple stress are not affected by the frictional coefficient.
- Substantial effect of irregularity factor has been observed on normal stress, shear stress and tangential couple stress. Specifically, as irregularity prevails in the medium stresses increases. Moreover the rectangular irregularity has more favourable effect to the stresses than the parabolic irregularity of same depth and span.
- Maximum depth of irregularity has remarkable effect on all the three stresses. All the three stresses increases with increase in the maximum depth of irregularity.
- For a particular depth of irregularity, it is observed that the stresses decreases abruptly with depth when depth is lesser than the maximum depth of the considered irregularity whereas stresses asymptotically approaches to zero when depth is higher than the maximum depth of the considered irregularity.

Acknowledgements

The authors convey their sincere thanks to respective institutes Thapar University, Patiala and Indian School of Mines, Dhanbad for providing us with its best facility for research. The authors also gratefully acknowledge Indian School of Mines, Dhanbad for providing JRF to Mr. Mriganka Shekhar Chaki.

References

Eringen, A.C. (1971), "Micropolar elastic solids with stretch", *Ari Kitap Evi Matbassi*, **24**, 1-18.

Iesan, D. and Pompei, A. (1995), "On the equilibrium theory of microstretch elastic solids", *Int. J. Eng. Sci.*, **33**, 399-410.

Tomar, S.K. and Monica, G. (2005), "Reflection and transmission of waves from a plane interface between two microstretch solid half spaces", *Int. J. Eng. Sci.*, **43**, 139-169.

Forest, S. and Sievert, R. (2006), "Non-linear microstrain theories", *Int. J. Solid. Struct.*, **43**, 7224-7245.

Sharma, V. and Kumar, S. (2016), "Influence of microstructure, heterogeneity and internal friction on SH waves propagation in a viscoelastic layer overlying a couple stress substrate", *Struct. Eng. Mech.*, **57**(4), 703-716.

Sharma, J.N., Kumar, S. and Sharma, Y.D. (2007), "Propagation of Rayleigh surface waves in microstretch thermoelastic continua under inviscid fluid loadings", *J. Therm. Stress.*, **31**, 18-39.
Cole, J. and Huth, J. (1958), "Stresses produced in a half plane by moving loads", *J. Appl. Mech.*, **25**, 433-436.
Craggs, J.W. (1960), "One two-dimensional wave in an elastic half plane", *Proceedings of the Cambridge Philosophical Society*, **56**, 269-275.
Sneddon, I.N. (1952), "Stress produced by a pulse of pressure moving along the surface of semi-infinite solid", *Rend Del Circ Matem di Paler*, **2**, 57-62.
Mukherjee, S. (1969), "Stresses produced by a load moving over a rough boundary of a semi-infinite transversely isotopic solid", *Pure Appl. Geophys.*, **72**, 45-50.
Sackman, J.L. (1961), "Uniformly moving load on a layered half plane", *J. Eng. Mech. Div. Proc.*, ASCE, 75-89.
Miles, I.W. (1966), "Response of a layered half space to a moving load", *J. Appl. Mech.*, **33**, 680-681.
Achenbach, J.D., Keshava S.P. and Herrmann, G. (1967), "Moving load on a plate resting on an elastic half space", *J. Appl. Math. Mech.*, **34**, 910-914.
Chonan, S. (1976), "Moving load on a pre-stressed plate resting on a fluid half-space", *Arch. Appl. Mech.*, **45**, 171-178.
Ungar, A. (1976), "Wave generation in an elastic half-space by a normal point load moving uniformly over the free surface", *Int. J. Eng. Sci.*, **14**, 935-945.
Olsson, M. (1991), "On the fundamental moving load problem", *J. Sound Vib.*, **145**, 299-307.
Lee, H.P. and Ng, T.Y. (1994), "Dynamic response of a cracked beam subject to a moving load", *Acta Mechanica*, **106**, 221230.
Alekseyeva, L.A. (2007), "The dynamics of an elastic half-space under the action of a moving load", *J. Appl. Math.*, **71**, 511-518.
Mukhopadhyay, A. (1965), "Stress produced by a normal moving load over a transversely isotropic layer of ice lying on a rigid foundation", *Pure Appl. Geophys.*, **60**, 29.
Selim, M.M. (2007), "Static deformation of an irregular initially stressed medium", *Appl. Math. Comput.*, **188**, 1274-1284.
Chattopadhyay, A. and Saha, S. (2006), "Dynamic response of normal moving load in the plane of symmetry of a monoclinic half space", *Tamkang J. Sci. Eng.*, **9**, 307.
Chattopadhyay, A., Gupta, S., Sharma V.K. and Pato Kumari (2011), "Stresses produced on a rough irregular half-space by a moving load", *Acta Mechanica*, **221**, 271-280.
Singh, A.K, Kumar, S. and Chattopadhyay, A. (2014), "Effect of irregularity and heterogeneity on the stresses produced due to a normal moving load on a rough monoclinic half-space", *Meccanica*, **49**(12), 2861-2878.
Kaur, T., Sharma S.K. and Singh, A.K. (2015), "Dynamic response of moving load on a micropolar half-space with irregularity", *Appl. Math. Model.*, doi:10.1016/j.apm.2015.09.102.
Szyiko-Bigus, O. and Sniady, P. (2015), "Dynamic response of a Timoshenko beam to a continuous distributed moving load", *Struct. Eng. Mech.*, **54** (4), 771-792.
Zhu, H., Mao, L., Weng, S. and Xia, Y. (2015), "Structural damage and force identification under moving load", *Struct. Eng. Mech.*, **53** (2), 261-276.
Kaur, T., Singh, A.K., Chattopadhyay, A. and Sharma, S.K. (2016), "Dynamic response of normal moving load on an irregular fiber-reinforced half-space", *J. Vib. Control*, **22**(1), 77-88.
Lin, G., Zhang, P., Liu, J. and Wang, W. (2016), "Elastic solutions due to a time-harmonic point load in isotropic multi-layered media", *Struct. Eng. Mech.*, **57**(2), 327-355.
Eringen, A.C. (1990), "Theory of thermomicrostretch elastic solids", *Int. J. Eng. Sci.*, **28**, 1291-1301.
Singh, B. and Kumar, R. (1998), "Wave propagation in a generalized thermomicrostretch elastic solid", *Int. J. Eng. Sci.*, **36**, 891-912.

Appendix 1

$$\xi_3=\frac{\lambda\left(\alpha_2q_2-\alpha_1q_1\right)+\lambda_0\left(\alpha_1q_1\beta_1-\alpha_2q_2\beta_2\right)}{\lambda\left(\alpha_1-\alpha_2\right)-\lambda_0\left(\alpha_1\beta_2-\alpha_2\beta_1\right)},\xi_4=\frac{\alpha_2^2q_2-\alpha_1^2q_1}{\lambda\left(\alpha_1-\alpha_2\right)-\lambda_0\left(\alpha_1\beta_2-\alpha_2\beta_1\right)},$$

$$\xi_5=\frac{\beta_2\xi_1q_1-\beta_1\xi_2q_2}{\beta_1\xi_2-\beta_2\xi_1},\xi_6=\frac{\beta_1\beta_2\left(q_1-q_2\right)}{\beta_1\xi_2-\beta_2\xi_1},\xi_7=\beta_1\xi_2-\beta_2\xi_1,\ \xi_8=\lambda\left(\alpha_1-\alpha_2\right)-\lambda_0\left(\alpha_1\beta_2-\alpha_2\beta_1\right),$$

$$\xi_9=\frac{\xi_6\xi_1-\xi_5\beta_2}{\xi_7},\xi_{10}=\frac{\xi_5\beta_1-\xi_6\xi_1}{\xi_7},\xi_{11}=\frac{\xi_4\left(\lambda-\lambda_0\beta_2\right)+\xi_3\alpha_2}{\xi_8},\xi_{12}=-\frac{\xi_4\left(\lambda-\lambda_0\beta_1\right)+\xi_3\alpha_1}{\xi_8}.$$

Appendix 2

$$P'=\left(\mu+\frac{\kappa}{2}-\frac{\gamma}{j}\right)\left(\lambda+2\mu+\kappa-\frac{\gamma}{j}\right),Q'=\left(\mu+\frac{\kappa}{2}-\frac{\gamma}{j}\right)^2+\left(\lambda+2\mu+\kappa-\frac{\gamma}{j}\right)^2+\left(\lambda+2\mu+\frac{\kappa}{2}\right)^2,$$

$$q'^2=\frac{Q'\pm\sqrt{Q'^2-4P'^2}}{2P'},m_1'=\frac{\left(\lambda+2\mu+\frac{\kappa}{2}\right)q_1'}{\left(\lambda+2\mu+\kappa\right)q_1'^2+\rho V^2-\mu-\frac{\kappa}{2}},m_2'=\frac{\left(\lambda+2\mu+\frac{\kappa}{2}\right)q_2'}{\left(\lambda+2\mu+\kappa\right)q_2'^2+\rho V^2-\mu-\frac{\kappa}{2}},$$

$$\alpha_1'=\frac{m_1'+q_1'}{2},\alpha_2'=\frac{m_2'+q_2'}{2},\xi_1'=q_1'\left(\kappa-\mu\right)+m_1'\mu-\kappa\alpha_1,\xi_2'=q_2'\left(\kappa-\mu\right)+m_2'\mu-\kappa\alpha_2,$$

$$\xi_3'=\frac{\lambda\left(\alpha_2'q_2'-\alpha_1'q_1'\right)}{\lambda\left(\alpha_1'-\alpha_2'\right)},\xi_4'=\frac{\left(\alpha_2'^2q_2'-\alpha_1'^2q_1'\right)}{\lambda\left(\alpha_1'-\alpha_2'\right)},\xi_8'=\lambda\left(\alpha_1'-\alpha_2'\right),\xi_{11}'=\frac{\xi_4'\lambda+\xi_3'\alpha_2'}{\xi_8'},\xi_{12}'=\frac{\xi_4'\lambda+\xi_3'\alpha_1'}{\xi_8'}.$$

Appendix 3

$$P''=\mu\left(\lambda+2\mu\right),Q''=\mu+\left(\lambda+2\mu\right)^2+\left(\lambda+\mu\right)^2,q''^2=\frac{Q''\pm\sqrt{Q''^2-4P''^2}}{2P''},$$

$$m_1''=\frac{\left(\lambda+\mu\right)q_1''}{\left(\lambda+2\mu\right)q_1'^2+\rho V^2-\mu},m_2''=\frac{\left(\lambda+\mu\right)q_2''}{\left(\lambda+2\mu\right)q_2'^2+\rho V^2-\mu},\ \alpha_1''=\frac{m_1''+q_1''}{2},\alpha_2''=\frac{m_2''+q_2''}{2},$$

$$\xi_1''=-q_1''\mu+m_1''\mu,\xi_2'=-q_2''\kappa+m_2''\mu,\xi_8'=\lambda\left(\alpha_1''-\alpha_2''\right),\xi_{11}'=\frac{\xi_4''\lambda+\xi_3''\alpha_2''}{\xi_8''},\xi_{12}'=-\frac{\xi_4''\lambda+\xi_3''\alpha_1''}{\xi_8''}$$